



*Supplement of*

## **Western European emission estimates of CFC-11, CFC-12 and CCl<sub>4</sub> derived from atmospheric measurements from 2008 to 2021**

**Alison L. Redington et al.**

*Correspondence to:* Alison L. Redington ([alison.redington@metoffice.gov.uk](mailto:alison.redington@metoffice.gov.uk))

The copyright of individual parts of the supplement might differ from the article licence.

*Copyright statement.* The works published in this journal are distributed under the Creative Commons Attribution 4.0 License. This licence does not affect the Crown copyright work, which is re-usable under the Open Government Licence (OGL). The Creative Commons Attribution 4.0 License and the OGL are interoperable and do not conflict with, reduce or limit each other. © Crown copyright 2023

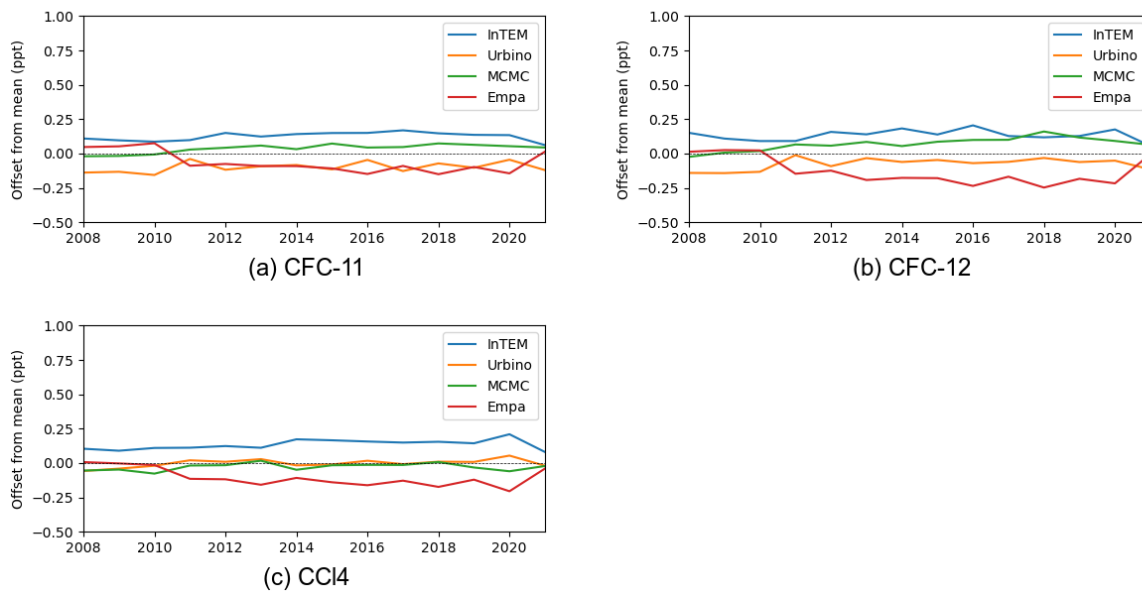


**Figure S1.** Annual average model offset from the four-model average of the posterior baselines at MHD for a) CFC-11, b) CFC-12 and c) CCl<sub>4</sub>

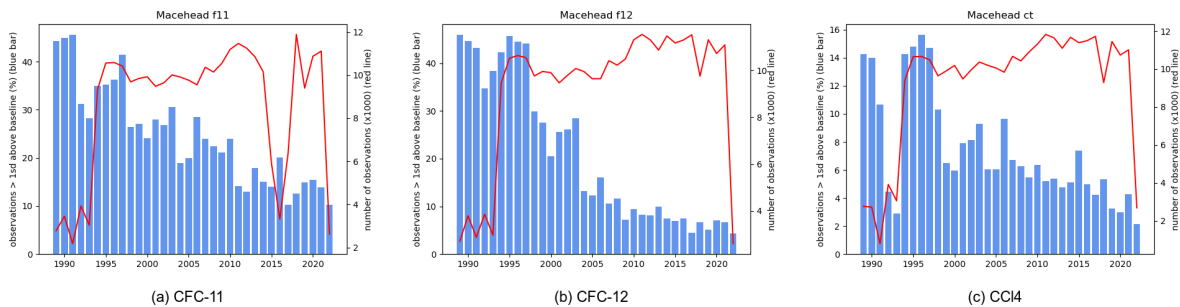


**Figure S2.** Percentage of total observations per year that are greater than either 1 standard deviation of the baseline and/or twice the instrument precision (blue bars) and total number of observations per year (red line) at MHD for a) CFC-11, b) CFC-12 and c) CCl<sub>4</sub>

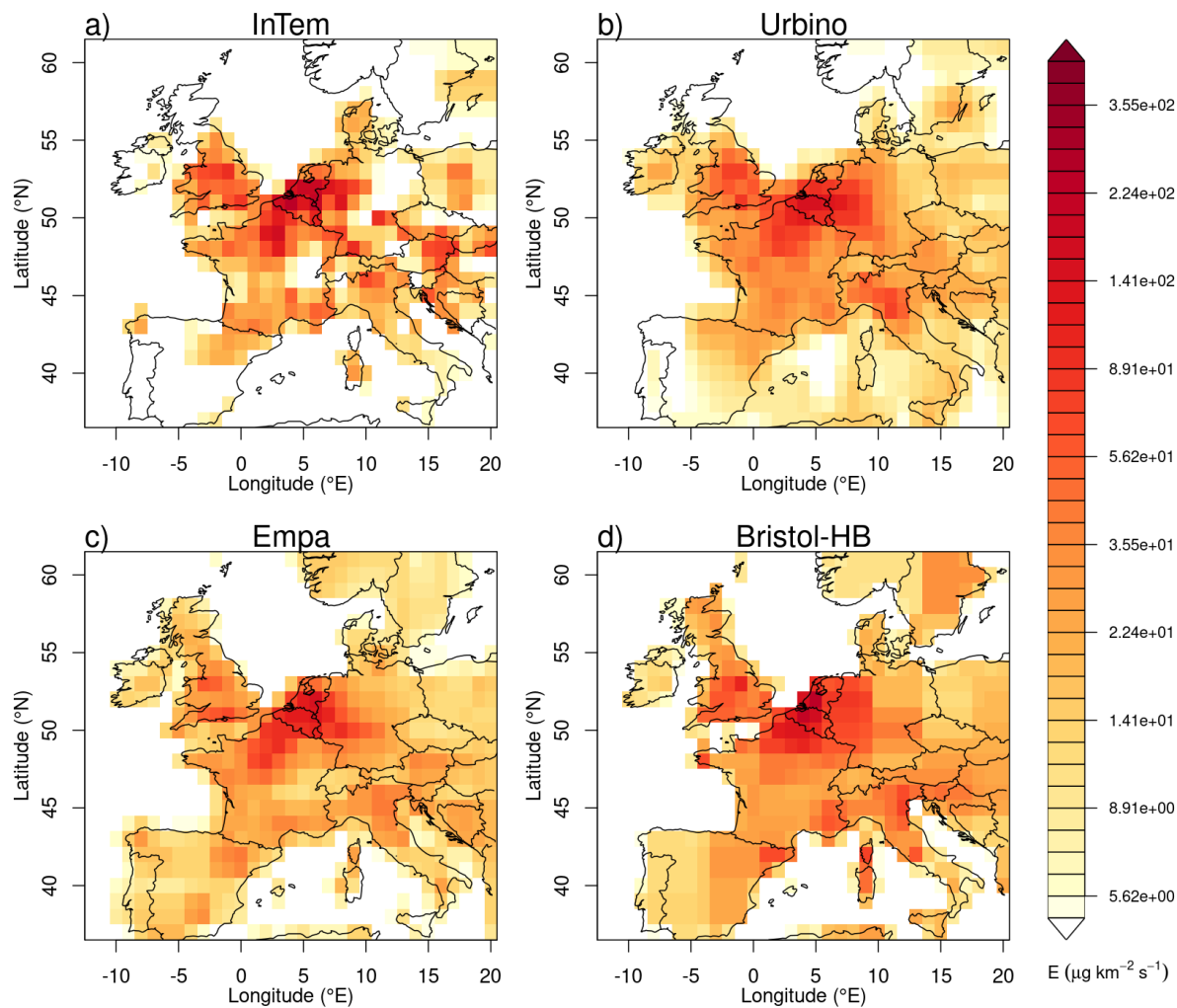


**Figure S3.** Average a posteriori CFC-11 emissions for the period 2013 to 2021 as estimated when using a flat a priori distribution and by the four inversion systems: a) InTEM, b) University of Urbino, c) Empa, d) Bristol-HB. Each of the inversion systems used a different irregular inversion grid, these were re-sampled here to a regular grid to allow for a more direct comparison.

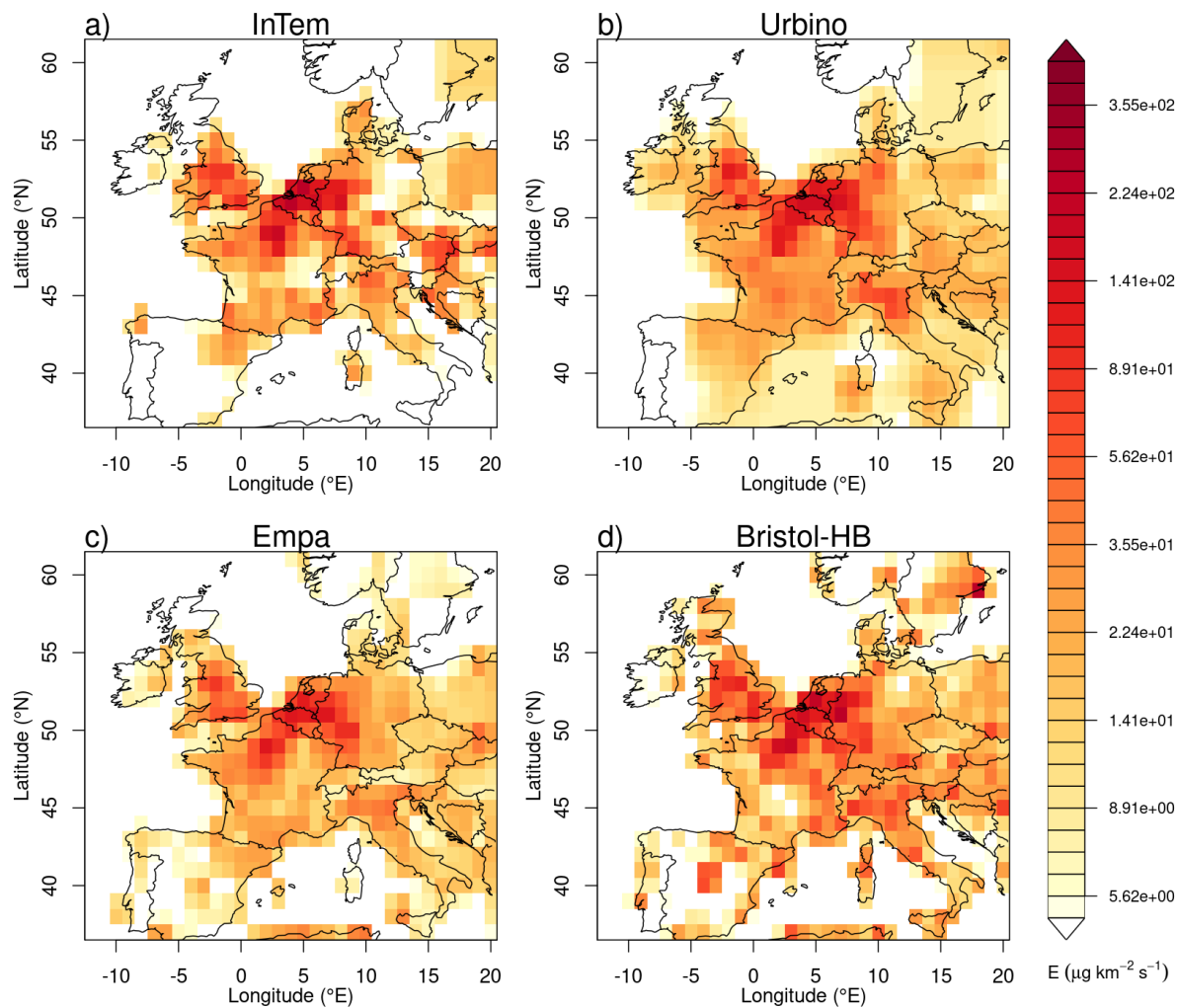


**Figure S4.** Average a posteriori CFC-11 emissions for the period 2013 to 2021 as estimated when using a population-based a priori distribution and by the four inversion systems: a) InTEM, b) University of Urbino, c) Empa, d) Bristol-HB. Each of the inversion systems used a different irregular inversion grid, these were re-sampled here to a regular grid to allow for a more direct comparison.

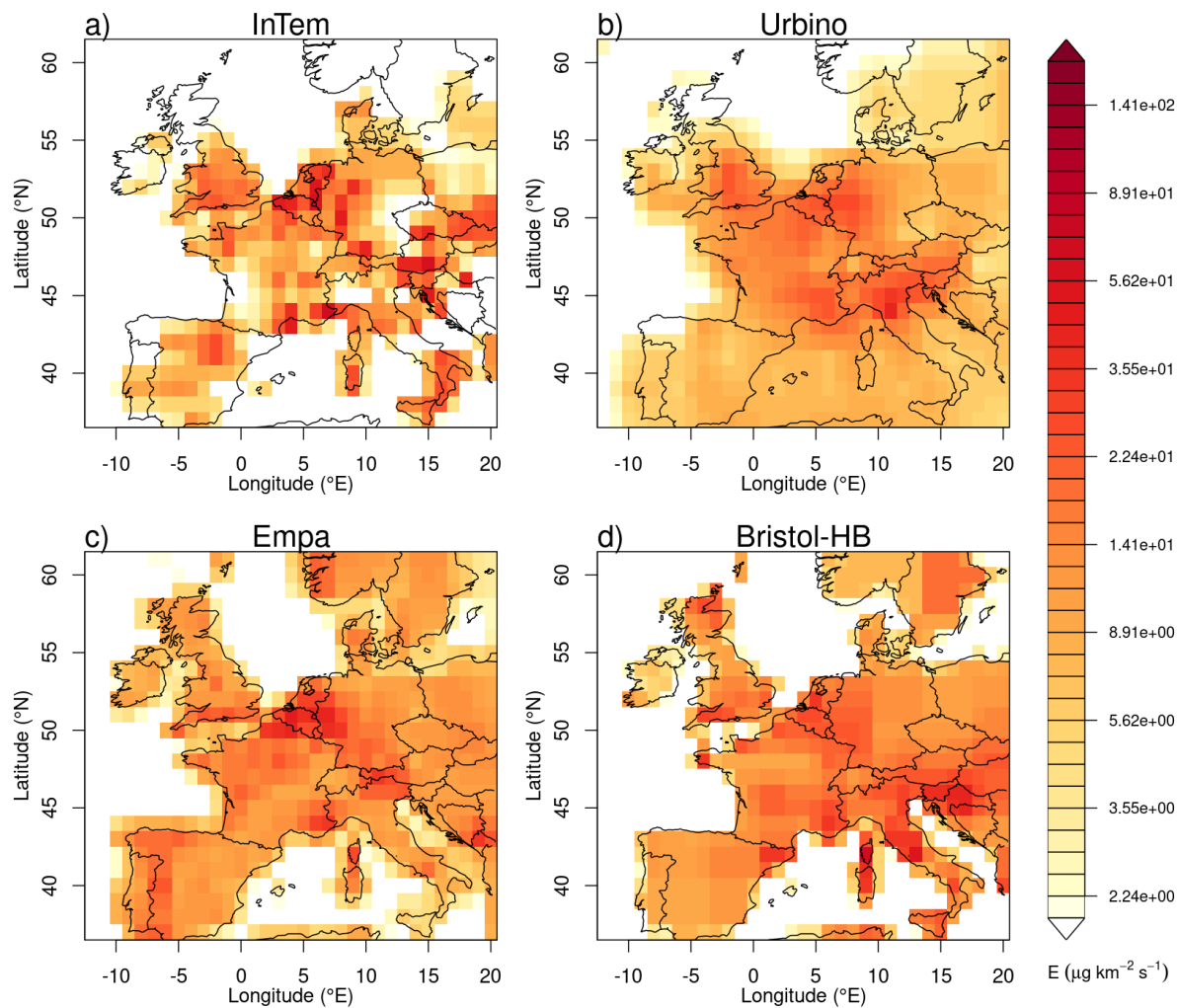


**Figure S5.** Average a posteriori CFC-12 emissions for the period 2013 to 2021 as estimated when using a flat a priori distribution and by the four inversion systems: a) InTEM, b) University of Urbino, c) Empa, d) Bristol-HB. Each of the inversion systems used a different irregular inversion grid, these were re-sampled here to a regular grid to allow for a more direct comparison.

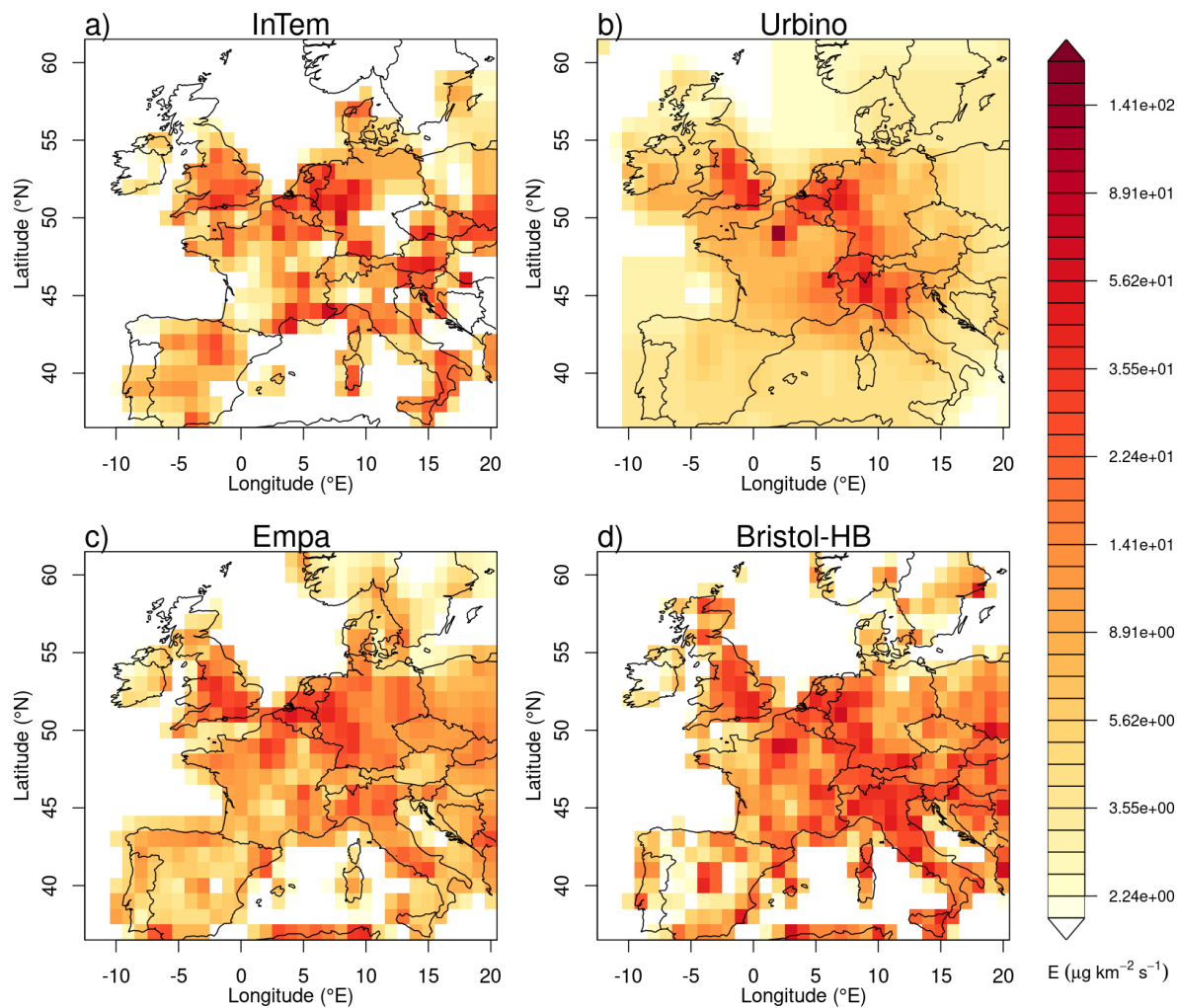


**Figure S6.** Average a posteriori CFC-12 emissions for the period 2013 to 2021 as estimated when using a population-based a priori distribution and by the four inversion systems: a) InTEM, b) University of Urbino, c) Empa, d) Bristol-HB. Each of the inversion systems used a different irregular inversion grid, these were re-sampled here to a regular grid to allow for a more direct comparison.

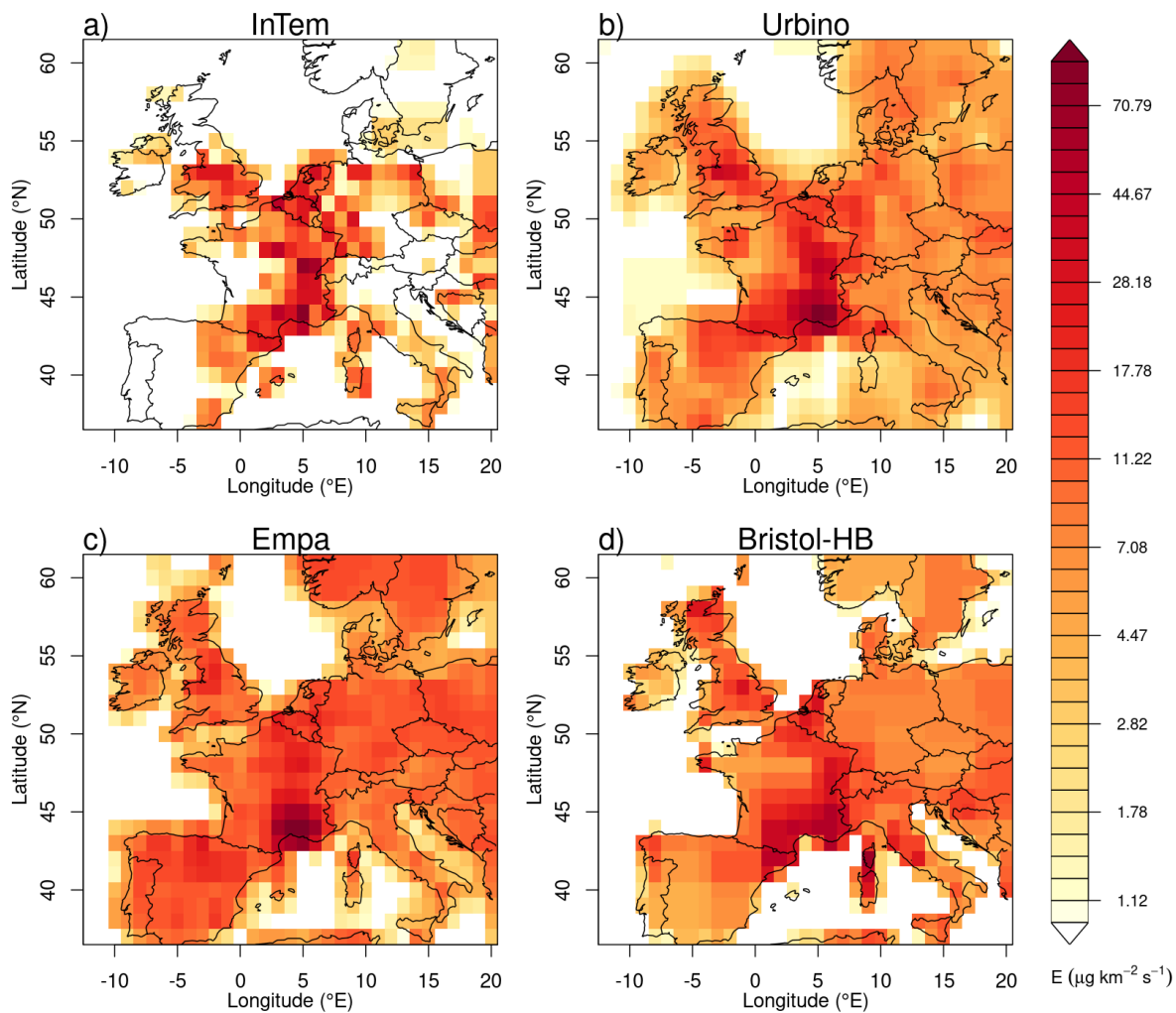


**Figure S7.** Average a posteriori  $\text{CCl}_4$  emissions for the period 2013 to 2021 as estimated when using a flat a priori distribution and by the four inversion systems: a) InTEM, b) University of Urbino, c) Empa, d) Bristol-HB. Each of the inversion systems used a different irregular inversion grid, these were re-sampled here to a regular grid to allow for a more direct comparison.



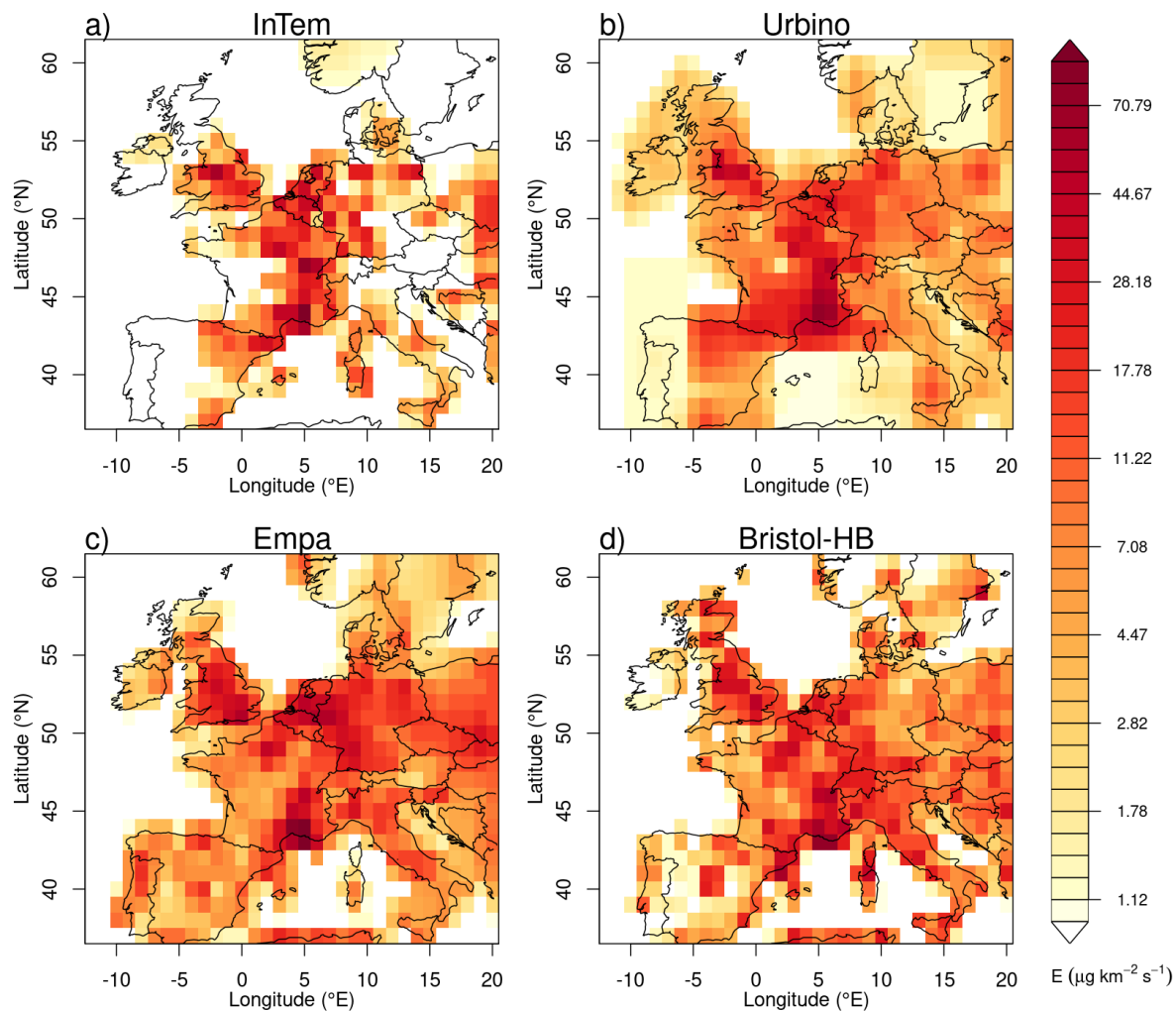


**Figure S8.** Average a posteriori CCl<sub>4</sub> emissions for the period 2013 to 2021 as estimated when using a population-based a priori distribution and by the four inversion systems: a) InTEM, b) University of Urbino, c) Empa, d) Bristol-HB. Each of the inversion systems used a different irregular inversion grid, these were re-sampled here to a regular grid to allow for a more direct comparison.

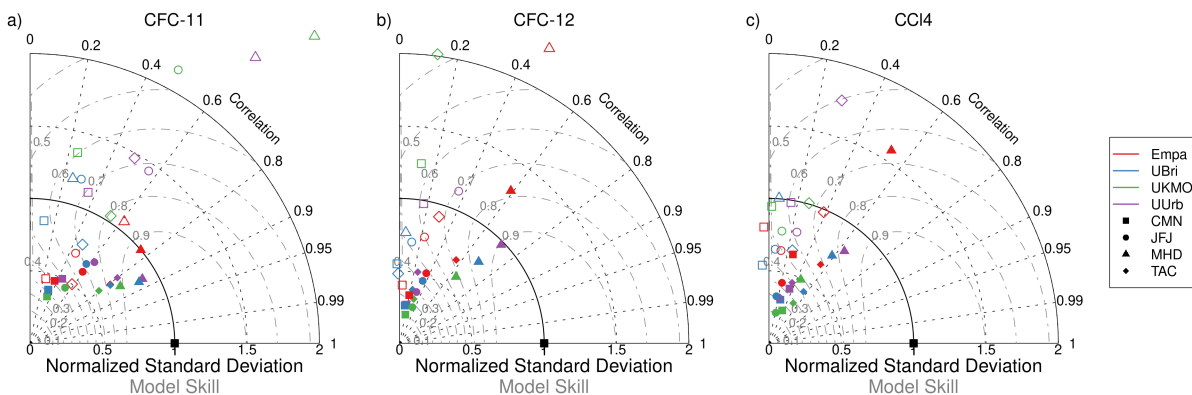


**Figure S9.** Model performance visualised in terms of Taylor diagrams, combining correlation coefficient and normalised standard deviation. Comparison statistics were calculated for the complete time series (2013 to 2021) of the regional concentration signals (observation minus baseline) at the four sites and daily aggregates: a) CFC-11, b) CFC-12, c) CCl<sub>4</sub>. Solid symbols identify a posteriori and open symbols a priori results. Different colours identify the model systems and different symbols the observation sites.

### S1 Bank Release Rate Calculation

5 We started with the assumption that all the emissions were from banks. We calculated the average 4-model emission for the period 2008-2021, giving a mid point of 2014. Initially assuming the average bank release rate from TEAP<sup>1</sup>, 2019 of 2.85%, we extrapolated backwards and forwards from this mid-2014 emission to give annual values for 2008-2021 inclusive. These annual values were compared with the modelled data using root mean square error (rmse). This process was repeated using

10 values in the range (1.5-4.2 %) given by TEAP, 2019. The minima rmse for the 4-model average results occurred at a bank release rate of 3.4 % for CFC-11. In order to establish a range of possible outcomes we repeated the process for the 4 models individually and calculated a bank release rate range of 2.6-4.5 %. (InTEM 2.6 %, MCMC 2.9 %, Urbino 4.5 %, Empa 3.6 %). The calculations were repeated for CFC-12.

<sup>1</sup>TEAP: Decisions XXX/3 TEAP Task Force Report on Unexpected Emissions of Trichlorofluoromethane (CFC-11), Tech. Rep., United Nations Environment Programme (UNEP), Nairobi, Kenya, [https://doi.org/ISBN\\_978-9966-076-78-6](https://doi.org/ISBN_978-9966-076-78-6), [https://ozone.unep.org/sites/default/files/2020-07/TEAP\\_Task\\_Force\\_Dec\\_XXX-3\\_on\\_Unexpected\\_CFC-11\\_Emissions\\_May\\_2019.pdf](https://ozone.unep.org/sites/default/files/2020-07/TEAP_Task_Force_Dec_XXX-3_on_Unexpected_CFC-11_Emissions_May_2019.pdf)